Synthesis and structure of a new oxynitride $Ba_3W_2O_6N_2$†

P. Subramanya Herle,[a] M. S. Hegde*[a] and G. N. Subbanna[b]

[a]*Solid State and Structural Chemistry Unit and*
[b]*Materials Research Centre, Indian Institute of Science, Bangalore, 560012, India*

A new oxynitride $Ba_3W_2O_6N_2$ has been synthesised from the ammonolysis of $Ba_3W_2O_9$. This compound crystallises in a hexagonal structure with $a=5.993(2)$ and $c=21.40(4)$ Å. Transmission electron microscopy (TEM) studies were carried out to elucidate the structure of this new compound. IR and Raman data are consistent with the C_{3v} site symmetry of the $(WO_3N)^{3-}$ unit. This compound is isostructural with $Ba_3V_2O_8$ reported in the literature.

In recent years there has been a spurt of interest in exploring new oxynitrides because of interesting structural and catalytic properties.[1,2] It has been known that oxygen atoms can substitute nitrogen atoms in monometallic nitrides due to similarity in their ionic radius as well as in polarizability. Of late a number of new ternary nitrides and oxynitrides have been discovered, *e.g.*, $LiMN_2$ (M=Mo,W),[3,4] $Mn_2(MnTa_3)N_{6-\delta}$ ($0\leqslant\delta\leqslant1$)[5] and $Ln_2Ta_2O_5N_2$ (Ln=lanthanide).[6] Bimetallic oxynitrides containing strongly electropositive elements such as $LaTaO_2N$, Na_3WO_3N[7] have substantial ionic character. Their limiting compositions have been described by the normal rule of valency.[8] There are reports on the ternary oxynitrides of rare-earths such as $Ln_2WO_{6-x}N_x$[9] and alkali-metal ions with tungsten. However, there are no reports on alkaline-earth metal and tungsten oxynitride phases. We wondered if partial substitution of N^{3-} for O^{2-} in the Ba–W–O system would yield any interesting material. Here we report our work on the synthesis and structure of the new oxynitride $Ba_3W_2O_6N_2$.

Experimental

The previously reported oxides $BaWO_4$, Ba_2WO_5, Ba_3WO_6 and $Ba_3W_2O_9$[10] were synthesised by taking stoichiometric amounts of BaO_2 (99.5%, Fluka) and WO_3 (99%, Koch Light) and heating in a muffle furnace and checking for product formation by powder X-ray diffraction. About 1.5 g of these oxides was loaded in a quartz tube in an alumina boat. The samples were heated in flowing ammonia gas (flow rate *ca.* 120 ml min^{-1}) at different temperatures. The products were analysed employing a JEOL-8P powder X-ray diffractometer (Cu-Kα radiation). The samples were heated in O_2 atmosphere in a temperature programmed reaction (TPR) system attached to a VG QXK300 quadrupole mass spectrometer[11] to check for nitride phase formation. In a typical experiment about 200 mg of the sample was loaded and the reactor was evacuated to 10^{-6} Torr. Oxygen gas was admitted at *ca.* 20–25 μmol s^{-1} and the reactor was heated from 30 to 700 °C at a rate of 15 °C min^{-1} and the gaseous products were analysed. Nitrogen estimation was carried out using a home-built thermogravimetric analyser. EDX analyses of these samples were conducted using a Cambridge scanning electron microscope (SEM) S-360, equipped with a LINK systems AN10000 X-ray analyser. FTIR spectra of the samples were recorded in polyethylene pellets in the range 100–700 cm^{-1} employing a Bruker IFS-113V FTIR spectrometer and a Nicolet Impact 400D FTIR instrument in the range 700–1400 cm^{-1} using KBr pellets. Raman spectra of the samples were recorded using a Spectra Physics SPEX 1403 double spectrometer (Ar-ion laser, $\lambda=$ 514.5 nm) series 2000. Electron diffraction and microscopy (TEM) were carried out using a JEOL 200CX transmission electron microscope to elucidate the microstructural features.

Results and Discussion

$BaWO_4$ was heated in ammonia at different temperatures. The product obtained when heated in ammonia at 900 °C for 12 h, was black and did not contain any starting material. The powder X-ray diffraction pattern of this sample (Fig. 1) was different from that of $BaWO_4$. When heated in O_2 atmosphere in the TPR system, this black material yielded only N_2 as the gaseous product. Since the sample was not highly crystalline and also because there was an indication of a small amount of a W_2N impurity phase, we were not sure whether the N_2 came from the W_2N phase alone or from any other unknown nitride product. To understand this reaction further, Ba_2WO_5 was heated in ammonia at 900 °C for 12 h. Interestingly, the powder pattern strongly resembles that of the black product obtained from $BaWO_4$ heated in ammonia. A small amount of W_2N impurity was also observed. From this it is clear that the starting oxide is decomposing to give rise to a new phase.

When Ba_3WO_6 was heated in ammonia, a white compound was obtained. The powder diffraction pattern of this compound contained the same unknown phase and BaO as impurity but there was no W_2N impurity. The TPR of oxidation of this white product gave N_2 as the gaseous product emanating above 375 °C. The amount of N_2 liberated was not as high as would be expected for a pure nitride phase indicating that the new phase is an oxynitride. From this it is clear that the unknown phase has a Ba/W composition between that of Ba_2WO_5 and Ba_3WO_6. When $Ba_3W_2O_9$ was heated in ammonia, a colourless single phase compound was obtained. This also liberated N_2 on heating in O_2. Experimental details

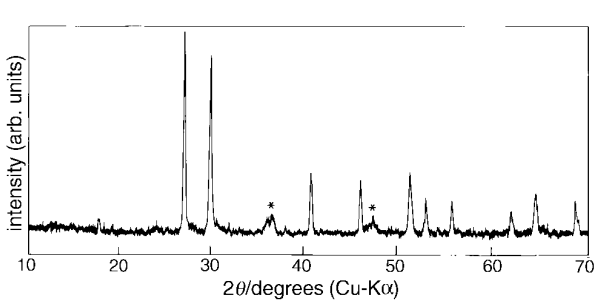

Fig. 1 Powder X-ray diffraction pattern of $BaWO_4$ heated in ammonia. The asterisks indicate W_2N impurity.

† Contribution no. 1263 from Solid State and Structural Chemistry Unit.

Table 1 Summary of ammonolysis of different ternary oxides

starting compound	ammonolysis conditions[a]	products
$BaWO_4$	900 °C	$Ba_3W_2O_6N_2 + W_2N$
Ba_2WO_5	900 °C	$Ba_3W_2O_6N_2 + W_2N$
Ba_3WO_6	900 °C	$Ba_3W_2O_6N_2 + BaO$
$Ba_3W_2O_9$	800 °C	$Ba_3W_2O_6N_2$
$Ba_3V_2O_8$	900 °C	no reaction

[a]Duration 12 h.

of all these studies are summarised in Table 1. When $Ba_3W_2O_9$ was heated at different temperatures, we found that the colour of the sample changed slowly from white to grey above 850 °C for 12 h. This colour change may be due to a partial reduction of W^{VI}. From this point, we focused our attention on the white product obtained from $Ba_3W_2O_9$. The powder X-ray diffraction pattern of this new phase is shown in Fig. 2 and the TPR of the new product in an oxygen atmosphere is shown in Fig. 3. We can see that the N_2 was liberated at 350 °C with simultaneous uptake of oxygen. The TG of this oxynitride

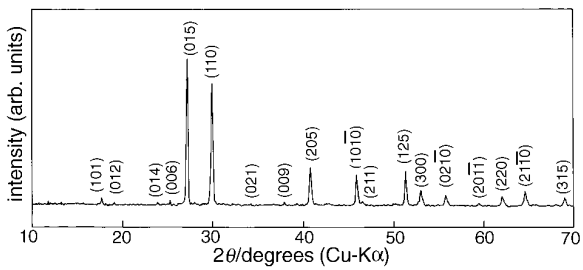

Fig. 2 Powder X-ray diffraction pattern of $Ba_3W_2O_6N_2$

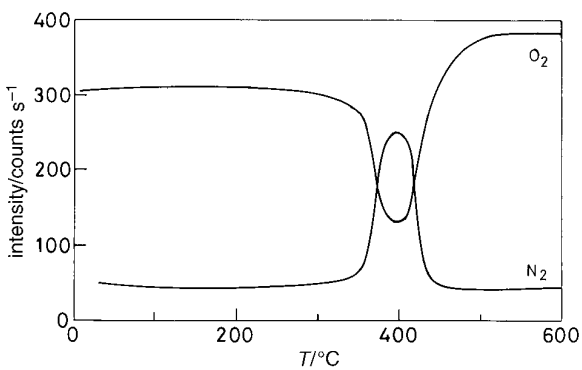

Fig. 3 TPR of oxidation of $Ba_3W_2O_6N_2$ in O_2

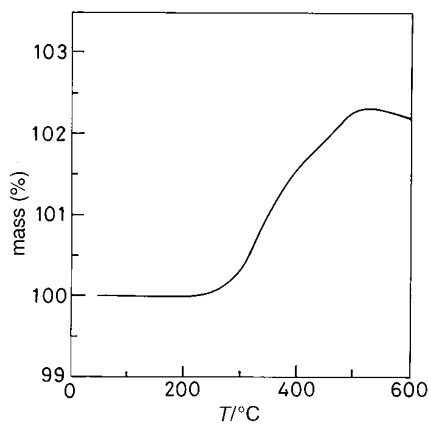

Fig. 4 TG of oxidation of $Ba_3W_2O_6N_2$

phase in oxygen atmosphere is shown in Fig. 4. The oxidised product contained a mixture of Ba_2WO_5 and $BaWO_4$ as the major phases and small amounts of $Ba_3W_2O_9$. There was a 2.2% mass gain in the TG experiment, which could be attributed to the loss of N_2 along with the uptake of oxygen. The molecular formula of the oxynitride from the TG studies is

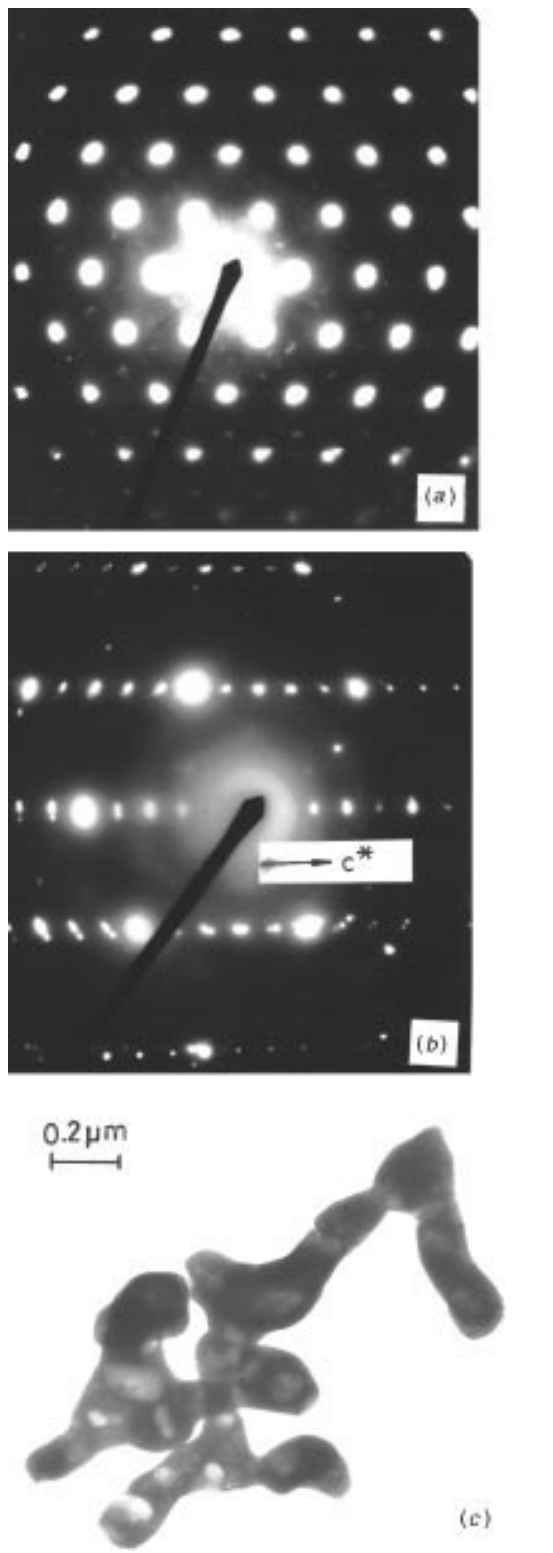

Fig. 5 (*a*) Electron diffraction pattern along the [0001] zone axis for $Ba_3W_2O_6N_2$; (*b*) electron diffraction pattern along the [01$\bar{1}$0] zone axis; (*c*) bright-field image of $Ba_3W_2O_6N_2$ crystallites

$Ba_3W_2O_6N_{2.00(\pm 0.01)}$. It is interesting that after the 2.2% mass gain, the sample started losing mass above 500 °C. Although the mass gain was expected, the mass loss could not be accounted for. To clarify this, $Ba_3W_2O_9$ was heated in flowing O_2 and it was found that this oxide does indeed lose mass above 500 °C, and gains its original mass on cooling.

Scanning electron microscopy (SEM) of these samples was conducted to confirm their metal composition. Spot mode analysis showed that the Ba/W ratio is 3:2. The above observations lead to the following chemical equations for the ammonolysis of $Ba_3W_2O_9$ and subsequent heating of the product in oxygen atmosphere:

$$Ba_3W_2O_9 + 4NH_3 \rightarrow Ba_3W_2O_6N_2 + 3H_2O + N_2 + 3H_2 \quad (1)$$

$$2Ba_3W_2O_6N_2 + 3O_2 \rightarrow 2Ba_2WO_5 + 2BaWO_4 + 2N_2 \quad (2)$$

All the peaks in the powder X-ray diffraction pattern (Fig. 2) could be indexed to a hexagonal cell with $a = 5.993(2)$ and $c = 21.40(4)$ Å. The intensity pattern of this sample was generated using the Lazy-Pulverix program with $Ba_3V_2O_8$[12] as the structural model. The observed and calculated intensity patterns of $Ba_3W_2O_6N_2$ are given in Table 2. The calculated intensities match the observed intensities quite well. For comparison powder diffraction data of $Ba_3V_2O_8$ is also given in Table 2.

Electron diffraction and microscopy was carried out in order to confirm the crystal structure of this phase. Fig. 5(*a*) and (*b*) show electron diffraction along [0001] and [01$\bar{1}$0] zone axes, confirming the hexagonal symmetry of the phase. The *d*-values obtained from electron diffraction agree with the observed *d*-parameters from the powder X-ray diffraction. Fig. 5(*c*) shows the bright field image of the powder particles. The particles are in the range of submicrometre regime with irregular morphology.

$Ba_3W_2O_9$ belongs to the B cation vacancy-ordered perovskite system with 2/3 of the octahedral sites in every layer filled with tungsten ions.[10] It can be recalled that, for $Ba_3W_2O_9$, the $(W_2O_9)^{6-}$ unit is in D_3 symmetry and the tungsten trigonal prisms share faces. However, in the case of $Ba_3V_2O_8$, vanadium ions are in tetrahedral coordination and there is no bridging oxygen between the two tetrahedra. In $Ba_3W_2O_6N_2$, the $(WO_3N)^{3-}$ unit should be in tetrahedral coordination and therefore the local site group of tungsten tetrahedra is assumed to be C_{3v}. To elucidate the local site geometry of oxide and nitride ligands around the tungsten atom, FTIR and Raman spectroscopic investigations were carried out for these samples. Fig. 6 shows the FTIR spectra of the $Ba_3W_2O_9$ and $Ba_3W_2O_6N_2$ phases. The IR spectrum of $Ba_3W_2O_9$ matches very well with the reported spectrum.[10] The bands in the region 1000–650 cm^{-1} have been assigned to the terminal stretching modes and the region 650–450 cm^{-1} contains bridging stretching modes. The far-IR bands can be attributed to the bending modes.

Fig. 7(*a*), (*b*) and (*c*) show Raman spectra of $Ba_3W_2O_9$, $Ba_3V_2O_8$ and $Ba_3W_2O_6N_2$ respectively. The FTIR and Raman spectra of the oxynitride closely resemble those of the $Ba_3V_2O_8$ phase. There are no bands in the region 650–450 cm^{-1}, which means that there are no bridging modes in the oxynitride. This observation clearly confirms that the bridging oxygen atoms were lost during the reaction and that the nitridation process is not topotactic in nature because the local coordination geometry around tungsten is completely changed. On the basis of intensities and on comparison with the spectra of $(MO_3N)^{n-}$ molecules (M = Re and Os),[13,14] we assign these bands to fundamentals of the $(WO_3N)^{3-}$ unit. According to the irreducible representations of the C_{3v} point group, $\Gamma = 3A_1 + 3E$. All

Table 2 X-Ray powder diffraction data for $Ba_3W_2O_6N_2$ [cell parameters $a = 5.993(2)$, $c = 21.40(4)$ Å] and $Ba_3V_2O_8$ [cell parameters $a = 5.7845(1)$, $c = 21.317(1)$ Å][a]

	$Ba_3W_2O_6N_2$				$Ba_3V_2O_8$	
h k l	d_{obs}/Å	d_{calc}/Å	I/I_0(obs.)	I/I_0 (calc.)	d_{obs}/Å	I/I_0 (obs.)
0 0 3	7.131	7.136	1	<1	7.09	4
1 0 1	5.039	5.057	5	6	4.878	11
0 1 2	4.670	4.680	2	2	4.537	3
0 1 4	3.738	3.731	<1	<1	3.651	12
0 0 6	3.560	3.568	3	3	—	—
0 1 5	3.302	3.306	100	100	3.247	100
1 1 0	2.998	3.005	89	90	2.893	75
0 2 1	2.585	2.583	2	1	2.487	4
2 0 2	—	2.528	—	<1	2.439	7
0 1 8	—	2.380	—	1	2.353	3
0 0 9	2.370	2.378	2	2	2.369	9
0 2 4	—	2.340	—	<1	2.267	11
1 1 6	—	2.298	—	<1	2.243	6
2 0 5	2.222	2.224	37	41	2.16	40
0 2 7	—	1.982	—	<1	1.934	4
1 0 10	1.980	1.980	21	24	1.962	25
2 1 1	1.951	1.959	6	9	1.886	3
1 2 2	1.923	1.934	2	5	—	—
1 1 9	—	1.865	—	<1	1.833	10
2 1 4	—	1.846	—	<1	1.785	3
1 2 5	1.787	1.787	19	17	1.731	25
3 0 0	1.733	1.735	14	18	1.670	13
0 2 10	1.653	1.653	11	12	1.624	12
1 2 8	—	1.585	—	<1	1.543	1
3 0 6	—	1.560	—	<1	1.511	2
2 0 11	1.559	1.558	1	3	—	—
2 2 0	1.503	1.502	11	15	1.446	10
2 1 10	1.448	1.448	12	9	1.416	13
1 3 1	—	1.440	—	<1	1.386	1
0 0 15	—	1.427	—	2	1.421	4
3 0 9	—	1.401	—	<1	1.3647	3
1 3 4	—	1.393	—	<1	1.3495	1
3 1 5	1.366	1.368	7	7	1.3208	9

[a]The values for $Ba_3V_2O_8$ are from JCPDS file 29–211.

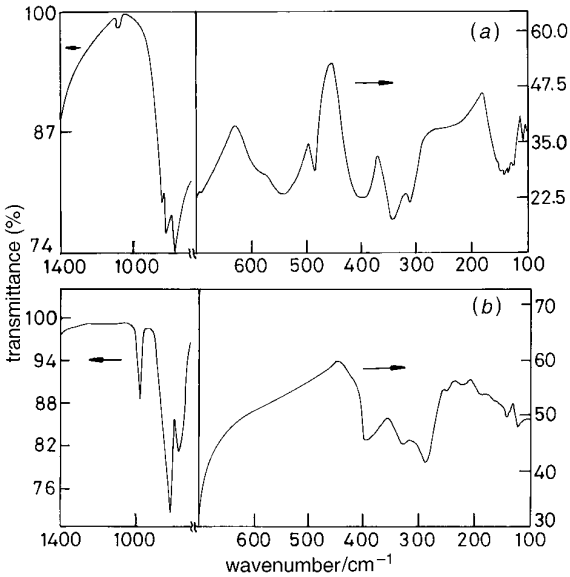

Fig. 6 FTIR spectra of (*a*) $Ba_3W_2O_9$ and (*b*) $Ba_3W_2O_6N_2$

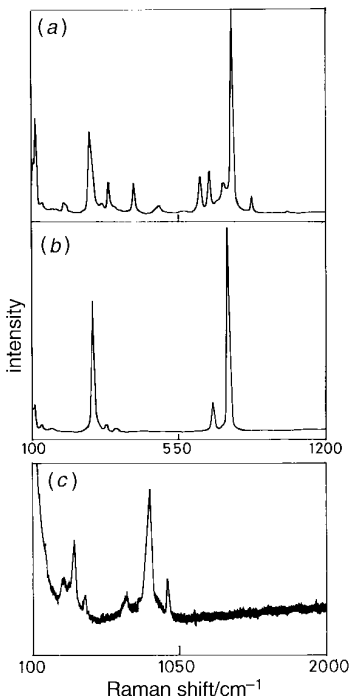

Fig. 7 Raman spectra of (*a*) $Ba_3W_2O_9$, (*b*) $Ba_3V_2O_8$ and (*c*) $Ba_3W_2O_6N_2$

these six modes are IR- and Raman-active. There are six IR and Raman bands in the region 100–1400 cm^{-1} clearly confirming the C_{3v} site symmetry of the $(WO_3N)^{3-}$ unit. We can assign the strong absorption band at 857 cm^{-1} [in Fig. 7(*c*)] to the symmetric stretching mode (ν_2). The less intense bands at 976, 707, 433, 370 and 296 cm^{-1} can be attributed to stretching (ν_1), antisymmetric stretching (ν_4) and three bending modes ν_6, ν_3 and ν_5. In the IR spectrum of $Ba_3W_2O_6N_2$, the broad unsymmetrical band centred around 350 cm^{-1} is composed of bands at 290, 340 and 391 cm^{-1} and three bands at 760, 815 and 983 cm^{-1} are assigned to ν_5, ν_3, ν_6, ν_4, ν_2 and ν_1 modes, respectively. The difference between FTIR and Raman spectra of the corresponding modes may be due to lack of coincidence arising from a coupling between the tetrahedral ions in the unit cell.[15] Our assignments also agree with the general rule that symmetrical stretch vibration gives the most intense Raman line.[16] Table 3 presents a comparison of IR spectrum of K_2ReO_3N and the Raman spectrum of $[OsO_3N]^{1-}$ ion in solution with the FTIR and Raman spectrum of $Ba_3W_2O_6N_2$. It is clear from the table that the transition-metal and the nitrogen ligand bond is stronger than the corresponding metal–oxygen bond. The general usefulness of vibration spectroscopy for confirmation and identification of structural features in polytypes of mixed metal oxides such as $Ba_3(B,B')_2O_{9-y}$ (B,B′ = Mo, W, V and Ti) has been systematically studied.[17] On the basis of above studies, we propose a structural model for this new oxynitride as shown in Fig. 8. From the literature we observe that in most of the oxynitrides which contain alkali/alkaline-earth metal the tetrahedrally coordinated transition metal in the highest possible oxidation state (*i.e.* Nb^V, Ta^V, Mo^{VI}, W^{VI}, Re^{VII} and Os^{VIII}). The stability

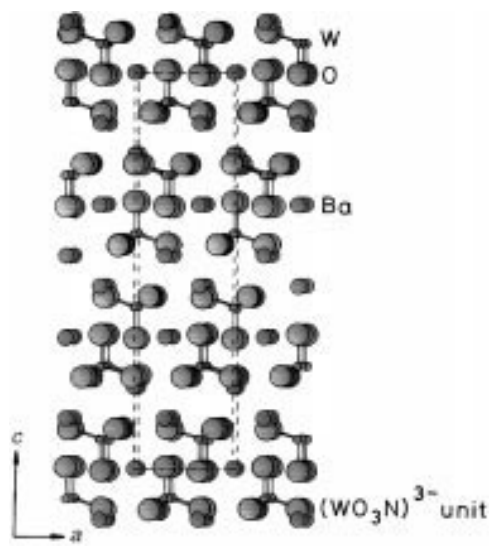

Fig. 8 Projection of $Ba_3W_2O_6N_2$ structure on the (010) plane emphasising the $(WO_3N)^{3-}$ tetrahedral polyanions. The unit cell is indicated by the dashed lines.

Table 3 Fundamental frequencies of vibration (cm^{-1}) of $(MO_3N)^{n-}$ (M = W, Re and Os) groups[a]

	assignment and description					
compound	$\nu_1(A_1)$ $\nu(M-N)$	$\nu_2(A_1)$ $\nu_s(MO_3)$	$\nu_3(A_1)$ $\delta(MO_3)$	$\nu_4(E)$ $\nu_{as}(MO_3)$	$\nu_5(E)$ $\delta(OMO)$	$\nu_6(E)$ $\delta(OMN)$
$K_2(ReO_3N)$ (IR solid)	1022	878	315	830	273	380
$Na(O_8O_3N)$ (R soln.)	1021	897	309	871	309	372
$Ba_3W_2O_6N_2$ (IR solid)	983	815	340	760	290	391
$Ba_3W_2O_6N_2$ (R solid)	976	857	370	707	296	433

R = Raman; soln. = solution.

of M^{n+} (M = transition metal) ion in the tetrahedral environment could be due to effective π bonding formation by the nitrogen atom in contrast with this type of bonding by the oxygen atoms. This is in agreement with predictions based on the simple consideration that, owing to the formal negative charge of N^{3-} and lower electronegativity of nitrogen than oxygen, N^{3-} will have greater tendency to donate electrons to the central metal atom through back bonding.[13]

It is interesting that when $Ba_3V_2O_8$ is heated in ammonia, there is no change in the powder diffraction pattern and also that there is no change in colour. This indicates a high thermodynamic stability of this oxide. The TPR of the product also did not show N_2 released from the sample. It is worth noting that, in the case of ammonolysis of $Ba_3W_2O_9$ and other barium tungsten oxide systems, $Ba_3W_2O_6N_2$ was the only stable phase obtained.

Attempts were made to obtain isostructural oxynitride phases containing molybdenum, $Sr_3W_2O_9$, $Sr_3Mo_2O_9$ and $Ba_3Mo_2O_9$ oxide phases not having been reported in the literature, in order to explore new possible oxynitrides belonging to $Ba_3W_2O_6N_2$ family. We prepared a series of oxide mixtures containing BaO_2, $Sr(NO_3)_2$ (Fluka, 99.5%), MoO_3 (Aldrich 99.9%) and WO_3 with (Ba,Sr):(Mo,W) in the ratio 3:2, and heated them to 600 °C for 24 h with intermittent grindings. Ammonolysis of these oxides was subsequently carried out at different temperatures and the products were analysed. Only for Ba–Mo oxide did X-ray patterns show the presence of an oxynitride phase related to $Ba_3W_2O_6N_2$ and $BaMoO_3$. In the other cases a perovskite-like phase was the major phase. It is known in the literature that the oxynitride $SrMoO_{2.6}N_{0.4}$[18] can be synthesised by heating $SrMoO_4$ in ammonia. For the $BaMoO_3$ related phase which we obtained as one of the product phases, it is quite possible that partial substitution of oxygen with nitrogen can take place.

Conclusions

We have synthesised a new oxynitride $Ba_3W_2O_6N_2$ from the ammonolysis of $Ba_3W_2O_9$ at 800 °C for 12 h. This confirms the generally observed trend that the ternary oxides containing the most electropositive ions (alkaline, alkaline earth, rare earth) will not form ternary nitrides by ammonolysis. They will perhaps form oxynitrides, or decompose into the electropositive metal oxide and binary transition-metal nitride. From $Ba_3W_2O_9$ to $Ba_3W_2O_6N_2$ the coordination number around the W^{6+} atom changes from six to four and correspondingly, the local site group symmetry changes from D_3 to C_{3v}. This oxynitride is isostructural with the $Ba_3V_2O_8$ phase. The corresponding molybdenum analogue $Ba_3Mo_2O_6N_2$ was obtained but could not be synthesised in a pure form.

The authors thank Dr H. N. Vasan for collection of FTIR and Raman data of the samples. One of the authors (P. S. H.) thanks the Council of Scientific and Industrial Research (CSIR), New Delhi for a fellowship. Financial support from the Department of Science and Technology, Govt. of India is gratefully acknowledged.

References

1 Rainer Niewa and Herbert Jacobs, *Chem. Rev*., 1996, **96**, 2053.
2 S. Sellem, C. Potvin, J. M. Manoli, R. Contant and G. Djéga-Mariadassou, *J. Chem. Soc., Chem. Commun*., 1995, 359.
3 S. H. Elder, L. H. Doerrer, F. J. DiSalvo, J. B. Parise, D. Guyomard and J. M. Tarascon, *Chem. Mater*., 1992, **4**, 928.
4 P. Subramanya Herle, N. Y. Vasanthacharya, M. S. Hegde, J. Gopalakrishnan and G. N. Subbanna, *J. Solid State Chem*., 1994, **112**, 208.
5 J. Grins, P.-O. Käll and G. Svensson, *J. Solid State Chem*., 1995, **117**, 48.
6 F. Pors, R. Marchand and Y. Laurent, *J. Solid State Chem*., 1993, **107**, 39.
7 S. H. Elder, F. J. DiSalvo, J. B. Parise, J. A. Hriljac and J. W. Richardson, Jr., *J. Solid State Chem*., 1994, **108**, 73.
8 D. S. Bem and H.-C. Zur Loye, *J. Solid State Chem*., 1993, **104**, 467.
9 R. Marchand, P. Antoine and Y. Laurent, *J. Solid State Chem*., 1993, **104**, 34.
10 K. R. Poeppelmeier, A. J. Jacobson and J. M. Longo, *Mater. Res. Bull*., 1980, **15**, 339.
11 M. S. Hegde, S. Ramesh and G. S. Ramesh, *Proc. Indian Acad. Sci*. (*Chem. Sci*.), 1992, **104**, 591.
12 P. Süsse and M. J. Buerger, *Z. Kristallogr*., 1970, **131**, 161.
13 B. Krebs and A. Müller, *J. Inorg. Nucl. Chem*., 1968, **30**, 463.
14 L. A. Woodward, J. A. Creighton and K. A. Taylor, *Trans. Faraday Soc*., 1960, **56**, 1267.
15 R. H. Busey and O. L. Keller, Jr., *J. Chem. Phys*., 1964, **41**, 215.
16 K. Nakamoto, *Infrared and Raman Spectra of Inorganic and Co-ordination Compounds*, John Wiley & Sons Inc., New York, 3rd edn., 1978.
17 B. Mössner and S. Kemmler-Sack, *J. Less-Common Met*., 1985, **114**, 333.
18 Guo Liu, Xinhua Zhao and H. A. Eick, *J. Alloys Compd*., 1992, **187**, 145.

Paper 7/02969A; *Received* 30*th April*, 1997